

# The Effects of Short-Chain Branching and Comonomer Type on the Interfacial Tension of Polypropylene–Polyolefin Elastomer Blends

CRAIG J. CARRIERE, H. CRAIG SILVIS

Materials Research and Development Laboratory, Central Research and Development, The Dow Chemical Company, Midland, Michigan 48674

Received 28 August 1996; accepted 25 April 1997

**ABSTRACT:** The imbedded fiber retraction method was used to assess the effect of increasing octene content and comonomer type on the compatibility of polypropylene–polyolefin elastomer (PP–POE) blends via direct measure of the interfacial tension. The interfacial tension was found to decrease monotonically with increasing octene content from a starting value of  $1.5 \pm 0.16$  dyn cm at an initial octene level of 9% down to  $0.56 \pm 0.07$  dyn cm at an octene content of 24%. These effects can be interpreted in terms of the effective decrease in the molecular weight between chain ends for the branched POE materials. The experimental data were found to be described well by a modification of the empirical relationship used to describe the effect of molecular weight on the interfacial tension for linear materials. The power–law parameter was found to be numerically equivalent for that obtained for the molecular weight dependence of linear materials. The measured interfacial tension was also found to be dependent on the type of comonomer used in the PP–POE systems. The interfacial tension ranged from  $1.07 \pm 0.09$  dyn cm for a PP–POE system made using ethylene–propylene down to  $0.56 \pm 0.07$  dyn cm for a PP–POE made using ethylene–octene (24% octene). © 1997 John Wiley & Sons, Inc. *J Appl Polym Sci* **66**: 1175–1181, 1997

**Key words:** interfacial tension; polypropylene; polyolefin elastomer; short-chain branching

## INTRODUCTION

The physical and mechanical properties of polymer blends depend critically on the morphology of the immiscible domains that develop during blending and processing.<sup>1–3</sup> The morphology of such systems is controlled mainly by the viscosities of the two components and the interfacial tension between the phases at the processing temperature.<sup>4–8</sup> Control of the interfacial tension is criti-

cal to develop blend morphologies that will yield systems with consistent and acceptable mechanical properties. High interfacial tension will generally lead to discrete phases in the systems with poor interfacial and, consequently, poor mechanical properties. It is widely known that the presence of chain end groups will drastically reduce the interfacial tension.<sup>3</sup> The effect of molecular weight on the measured interfacial tension below the plateau region is generally interpreted to be due to the increased number of end groups present in the interfacial region.<sup>9–12</sup> A statistical thermodynamic theory proposed by Poser and Sanchez<sup>13,14</sup> which is based on the square gradient approach of Cahn and Hillard,<sup>15</sup> predicts that the molecular weight dependence of the surface and

Correspondence to: C. J. Carriere, Biomaterials Processing Research, National Center for Agricultural Utilization Research, Agricultural Research Service, United States Department of Agriculture, 1815 North University Street, Peoria, IL 61604.

*Journal of Applied Polymer Science*, Vol. 66, 1175–1181 (1997)  
© 1997 John Wiley & Sons, Inc. CCC 0021-8995/97/061175-07

interfacial tension should scale as  $M_n^{-2/3}$ . Kumar et al.<sup>16</sup> have shown that the exponential changes from  $\frac{2}{3}$  to 1 as the chain length increases due to the effects of end groups. The power-law exponent has been found experimentally to be equal to  $\frac{2}{3}$  for low-molecular-weight simple fluids such as *n*-alkanes and to range from  $\frac{1}{2}$  to 1 for polymeric materials.

The focus of this effort was to investigate the effect of short-chain branching and comonomer type on the measured interfacial tension of polypropylene–polyolefin elastomer (PP–POE) blends. The short chain branches were controlled by systematically increasing the octene level in the POE materials produced from ethylene–octene comonomers. The effect of comonomer type on the interfacial tension was studied by using POE materials produced from ethylene–propylene, ethylene–butene, ethylene–pentene, and ethylene–octene. The effects of short-chain branching and comonomer type were characterized by direct measurements of the interfacial tension using the imbedded fiber retraction (IFR) method.<sup>9,17–21</sup>

## EXPERIMENTAL METHODS

### Materials

The samples of POEs used in these studies were supplied by the Dow Chemical Company (Midland, MI). The POE materials produced using ethylene–octene comonomers were all of equivalent melt index ( $\approx 1.0$  dg min, ASTM D-1238, Condition E) and ranged in density from 0.870 g cc (24 wt % octene) to 0.910 g cc (9 wt % octene). The POE materials produced from ethylene–propylene, ethylene–butene, and ethylene–pentene comonomers were all of equivalent melt index ( $\approx 1.0$  dg min, Condition E) and density ( $\rho \approx 0.870$  g cc). The PP used was an isotactic homopolymer obtained from Montell Polyolefins (Houston, TX) designated as 6323 with a nominal 12 melt flow rate (ASTM D-1238, Condition L).

### Sample Fabrication

Pellets of the PP material were extruded into a fiber with a nominal 0.015 in. diameter. The pellets were charged into a modified Instron capillary rheometer warmed to  $200 \pm 3^\circ\text{C}$  and allowed to melt. The pellets were packed together using a metal rod as they melted in the capillary chamber. The material was extruded through a 0.015 in. circular die mounted below the capillary. The pis-

ton speed was maintained at 0.25 cm h to minimize any shear-induced stresses that could remain in the fiber as it exited the die and cooled to room temperature. The extruded fiber was collected as it exited the die over a 4-h period. Only fibers that were produced well into the extrusion process were used in the experiments to eliminate distortions in the specimens due to transient effects in the start-up of the flow. All the fibers were inspected after extrusion using a light microscope to ensure their uniformity.

Pellets of the various POE samples were molded into thin circular disks and used for both the IFR and zero-shear viscosity experiments. The pellets were compression molded at  $200 \pm 3^\circ\text{C}$  into disks 1 in. in diameter and 0.125 in. thick.

Sections of the PP fiber were cut using a razor to uniform lengths of approximately 0.15 in. This produced fiber specimens for the IFR experiments with nominal  $L/D$  (length/diameter) ratios of 10. Special care was exercised to ensure that the fiber and disk specimens were not contaminated with dirt or fingerprints. All the glassware, razor blades, and tweezers were routinely cleaned with acetone prior to specimen handling, and surgical gloves were worn during sample preparation.

The exact dimensions of each PP fiber used in the IFR experiments were determined by videotaping the fiber on top of a microscopic ruler. The fiber was then placed between two disks of the appropriate POE material and placed in the nitrogen-purged oven of the IFR apparatus.<sup>9,20</sup> The fiber was entombed in the POE matrix at  $150 \pm 1^\circ\text{C}$ . After the POE melt front enclosed the fiber, the composite samples were then annealed for an additional hour to ensure the removal of any residual stresses in the fiber due to processing. After the annealing treatment, the temperature was increased to  $200 \pm 1^\circ\text{C}$ , and the image was recorded as the shape evolution developed.

### Zero-Shear Viscosity Measurements

The zero-shear viscosities of all the materials were determined using a Rheometrics RDSII dynamic mechanical spectrometer. The experiments were conducted using parallel-plate fixtures at a temperature of  $200 \pm 1^\circ\text{C}$ . All the experiments were conducted under a dry nitrogen environment. The sample was subjected to a small-amplitude oscillatory shear flow in the linear viscoelastic regime at strains of 0.5% or less. Measurements were made for angular frequencies ranging from 0.01 to 100 rad s at 0.2 decade intervals. The

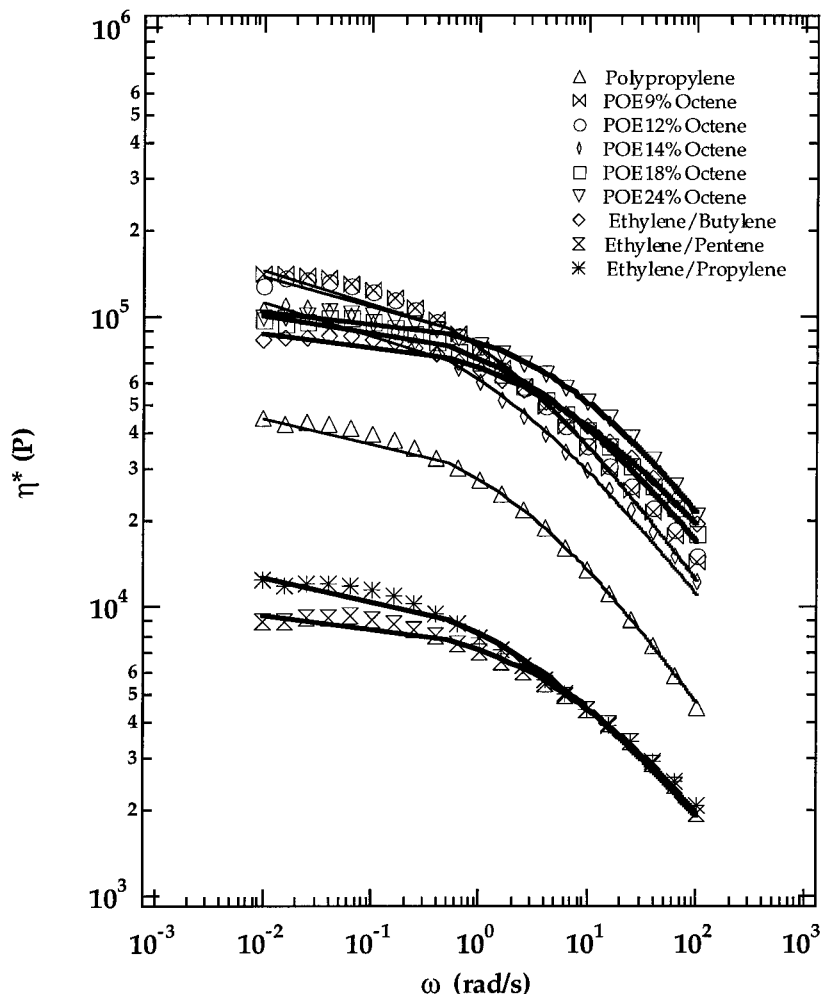


**Figure 1** Evaluation of the zero-shear viscosities at 200°C for the various POE materials studied as a function of octene content and comonomer type, along with PP. The solid lines are the model fits to the data using the Ellis equation. The parameters obtained using the equation are summarized in Table I.

data were subsequently transferred to a Macintosh computer. The zero-shear viscosity was obtained by fitting the rheological data to the Ellis model using custom fitting programs written in Igor Pro. The Ellis model can be expressed as

$$\eta = \frac{\eta_0}{1 + (\omega\tau)^b} \quad (1)$$

where  $\eta_0$  is the zero-shear viscosity,  $\omega$  is the angular frequency,  $\tau$  is the characteristic relaxation time constant, and  $b$  is a fitting parameter. The relative precision of the zero-shear viscosities was estimated at 5–10%. Plots of the experimental data, as well as the model fits, are illustrated in Figure 1. The results of the model fitting procedures are summarized in Table I.

### Interfacial Tension Measurements

PP-POE interfacial tensions were measured using the IFR method.<sup>9,17–21</sup> This method allows the molten polymer-polymer interfacial tension to be determined quantitatively by monitoring the shape evolution of a fiber of material. A imbedded in a matrix of material B. The IFR is a dynamic method and therefore does not face the limitations of traditional equilibrium experiments when applied to high-viscosity polymer melts.<sup>9,17–26</sup> The IFR apparatus has been discussed previously, and the reader is referred to the literature.<sup>9,20</sup> The method is applicable to nonreactive, immiscible, high-viscosity systems, such as molten high polymers. Interfacial tension serves as the driving force for the retraction process and is opposed

**Table I Summary of the Rheological Properties of the PP and Various POE Materials at 200°C**

Material	$\eta_0$ ( <i>P</i> )	$\tau$ (s <sup>-1</sup> )	<i>b</i>
Polypropylene	$4.66 \times 10^4$	0.53	0.55
POE, 9 wt % octene	$1.57 \times 10^5$	1.0	0.53
POE, 12 wt % octene	$1.47 \times 10^5$	0.82	0.55
POE, 14 wt % octene	$1.23 \times 10^5$	1.1	0.50
POE, 18 wt % octene	$1.04 \times 10^5$	0.24	0.52
POE, 24 wt % octene	$1.05 \times 10^5$	0.12	0.56
POE, ethylene-propylene	$1.3 \times 10^4$	0.44	0.48
POE, ethylene-butene	$8.9 \times 10^4$	0.13	0.51
POE, ethylene-pentene	$9.5 \times 10^3$	0.14	0.53

throughout the shape evolution by the viscous resistance of the two materials. The retraction process is observed to proceed with the fiber transformed from its initial cylindrical geometry, through a dumbbell-like intermediate, and finally to a sphere.<sup>17-19</sup> The mathematical development for this shape evolution has been discussed elsewhere.<sup>19</sup> Only a brief review of the analysis will be given here. The shape evolution is described by a one-dimensional equation in the normalized cylinder radius *r*, which can be expressed as

$$f(r) = 3 \ln \left[ \frac{(1+r+r^2)^{1/2}}{1-r} \right] + 3^{3/2} \arctan \left[ \frac{3^{1/2}r}{2+r} \right] - r - 8r^{-2} \quad (2)$$

where

$$r = \frac{R}{R_0} \quad (3)$$

The parameter *r* is evaluated at various times, *t*, throughout the retraction process. The value of *f*(*r*) is related to *t* through

$$f(r) = \lambda^{-1}t + f(r_e) \quad (4)$$

where

$$r_e = \frac{R_e}{R_0} \quad (5)$$

$$\lambda = \frac{\eta R_0}{\gamma_{12}} \quad (6)$$

and

$$\eta = \frac{\eta_m + \alpha\eta_f}{1 + \alpha} \quad (7)$$

In the expression referenced above, *R* is the absolute cylinder radius at time *t*, *R<sub>e</sub>* is the absolute cylinder radius at *t* = 0, and *R<sub>0</sub>* is the absolute cylinder radius at *t* = ∞. Typically, the quantity *R<sub>0</sub>* is determined from the initial fiber volume, *V*, through

$$R_0 = \left( \frac{3V}{4\pi} \right)^{1/3} \quad (8)$$

Equation (8) makes use of the observation that the final equilibrium shape of the fiber will be a sphere.<sup>17-20</sup> The effective viscosity  $\eta$  is given in terms of the zero-shear viscosities of the matrix,  $\eta_m$ , and the fiber,  $\eta_f$  as well as the constant  $\alpha$ , which has been determined to be 1.7.<sup>19</sup> The quantity  $\lambda$  is the characteristic time constant for the retraction process. The interfacial tension  $\gamma_{12}$  is obtained from the slope of the *f*(*r*) versus *t* plot, an example of which is shown in Figure 2.

## RESULTS AND DISCUSSION

The interfacial tensions for PP against each of the eight POE materials were measured at 200°C. The measured interfacial tensions between PP and the various POE materials are summarized in Table II. The precision of the data was evaluated from replicate runs and is reported as ±2 standard deviations.

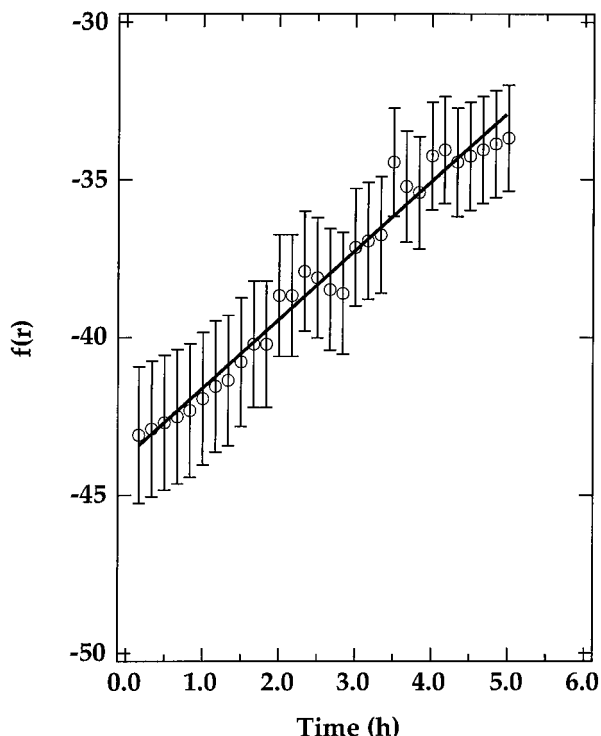


**Figure 2** Representative IFR data for PP-POE (9% octene) at 200°C. The interfacial tension is proportional to the slope of line fit through the experimental data.

The effect of increasing octene content in the POE used in the PP-POE system manifests itself in a decrease in the interfacial tension, as is illustrated in Figure 3. Higher levels of octene in the POE will thus lead to better compatibility between the two phases and should also lead to more uniform physical properties for the blends. The increase in octene content can also be examined as a decrease in the molecular weight between end groups. The effect of molecular weight on the

interfacial tension for linear materials has been described by the following empirical expression<sup>16-19</sup>:

$$\gamma_{12} = \gamma_{\infty} - \frac{k}{M_n^{-z}} \quad (9)$$

where the molecular weight of one of the components is varied. In eq. (9),  $\gamma_{\infty}$  is the infinite molecular weight limit,  $M_n$  is the number-average molecular weight, and  $k$  and  $z$  are fitting parameters. As discussed earlier, for polymeric materials,  $z$  typically has been found to range from  $\frac{1}{2}$  to 1. Equation (9) can be regarded as a special case of a more general expression where the molecular weight in the expression is the average molecular weight between chain ends. Thus, for branched system, it can be advanced that the interfacial tension should follow

$$\gamma_{12} = \gamma_{\infty} - \frac{k}{M_{n,b}^{-z}} \quad (10)$$

where  $M_{n,b}$  is the number-average molecular weight between branch points. It is expected that the exponential power  $z$  should cover a similar range to that found for linear polymeric materials. Making the assumption that the volume fraction of octene in the POE materials is proportional to the molecular weight between branch points, eq. (10) can be recast as

$$\gamma_{12} = \gamma_{\infty} - \frac{k'}{\phi_{\text{octene}}^{-z}} \quad (11)$$

where  $k'$  is a fitting constant, and  $\phi_{\text{octene}}$  is the volume fraction of octene in the POE materials.

**Table II** Interfacial Tension Values for the Various PP/POE Materials at 200°C

Sample	Absolute Fiber Length Prior to Retraction (cm)	Time of Retraction (h)	Interfacial Tension (dyn cm)
PP/POE, 9 wt % octene	0.151 ± 0.002	5	1.5 ± 0.16
PP/POE, 12 wt % octene	0.104 ± 0.002	5.75	1.01 ± 0.20
PP/POE, 14 wt % octene	0.103 ± 0.002	8	0.92 ± 0.16
PP/POE, 18 wt % octene	0.100 ± 0.002	6.25	0.71 ± 0.11
PP/POE, 24 wt % octene	0.102 ± 0.002	7.7	0.56 ± 0.07
PP/POE, ethylene-pentene	0.120 ± 0.002	retraction not observed	0.00 ± 0.08
PP/POE, ethylene-butene	0.137 ± 0.002	11	0.85 ± 0.13
PP/POE, ethylene-propylene	0.166 ± 0.002	16	1.07 ± 0.09

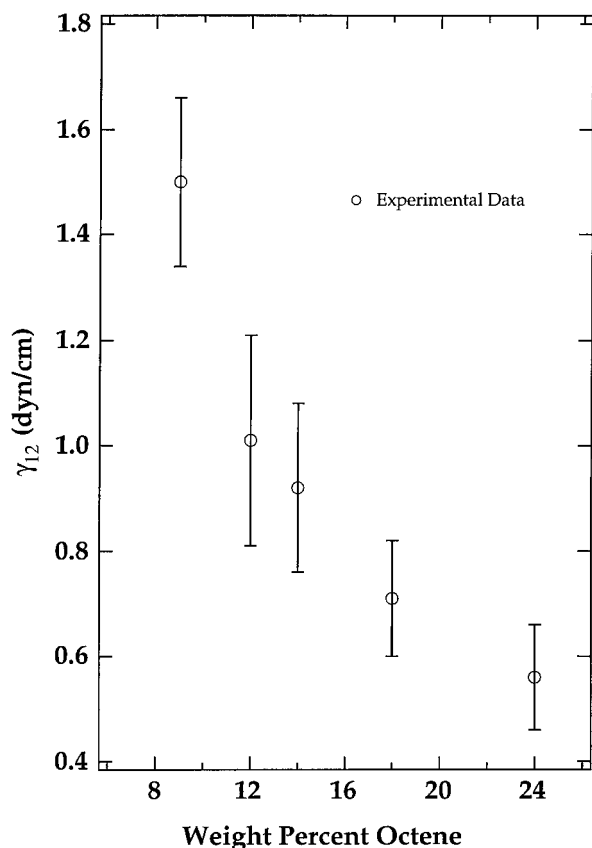


**Figure 3** Effect of octene content on the interfacial tension of PP-POE systems. The error bars represent  $\pm 2\sigma$  standard deviations.

The effect of short-chain branching on the interfacial tension is illustrated in Figure 4. The experimental data were fit using eq. (11). The best statistical fit was found with  $\gamma_{\infty} = 2.87 \pm 0.37$  dyn cm,  $k' = 4.6 \pm 0.2$ , and  $z = 0.45 \pm 0.17$ . It is interesting to note that the power-law exponent is within the range typically observed for linear materials. The value for the limiting interfacial tension yields a value for the interfacial tension of PP and linear POE. Due to the paucity of experimental data on the interfacial tension of high polymers in the literature, a direct comparison of this value is not currently possible.

The effect of the change in the comonomer type on the interfacial tension is illustrated in Figure 5. From the experimental data, it is evident that an increase in the length of the side chain from ethylene-propylene to ethylene-octene causes a statistically significant drop in the measured interfacial tension. This result indicates that PP-POE materials produced with ethylene-octene should be more compatible than those made with

either ethylene-butene or ethylene-propylene at the composition studied. The experiment run using ethylene-pentene did not exhibit any retraction of the fiber over a 24 h period. Instead, the fiber was observed to slowly disperse in the PP matrix. This observation indicates that the interfacial tension for this system is close to zero.

## CONCLUSIONS

The IFR method was used to assess the effect of increasing octene content and comonomer type on the compatibility of PP-POE blends via direct measure of the interfacial tension. The interfacial tension was found to decrease monotonically with increasing octene content from a starting value of  $1.5 \pm 0.16$  dyn cm at an initial octene level of 9% down to  $0.56 \pm 0.07$  dyn cm at an octene content of 24%. Increased octene level resulted in more compatible blends, as evidenced by the decrease in the interfacial tension. These effects can be interpreted in terms of the effective decrease in the

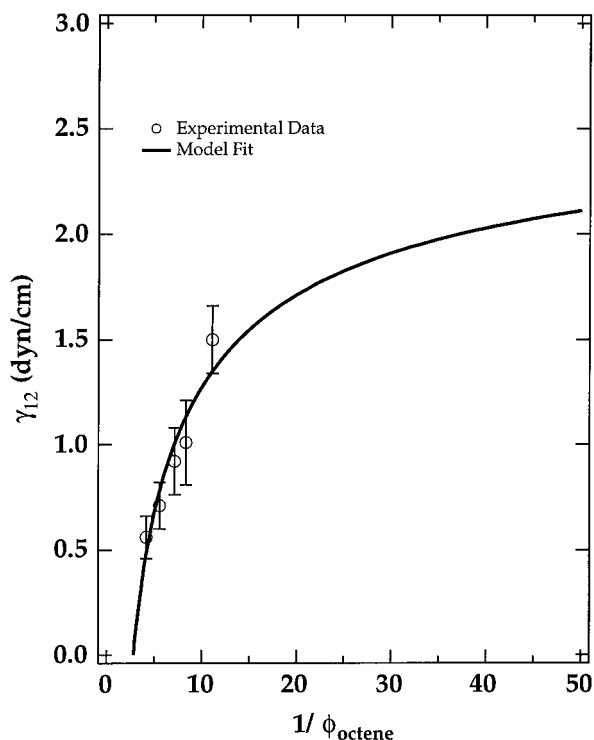


**Figure 4** The effect of short-chain branching on the interfacial tension of PP-POE (varying octene levels) materials at 200°C. The solid line is a model fit to the experimental data using eq. (11) in the text with  $\gamma_{\infty} = 2.87 \pm 0.37$  dyn cm,  $k' = 4.6 \pm 0.2$ , and  $z = 0.45 \pm 0.17$ .

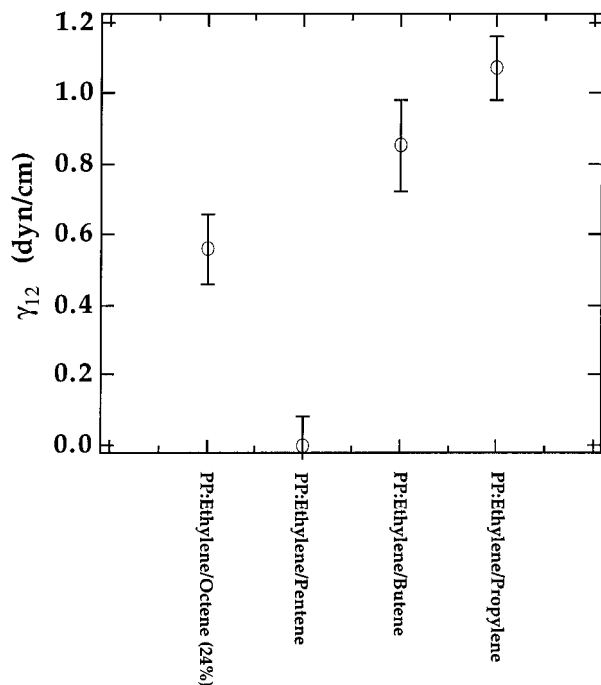


**Figure 5** Effect of side group type on the interfacial tension of PP-POE systems. The measurements were performed at 200°C, and the error bars represent  $\pm 2\sigma$ .

molecular weight between chain ends for the branched POE materials. Increasing octene levels lead to more chain ends per molecule and a lower average molecular weight between chain ends. The experimental data were found to be described well by a modification of the empirical relationship used to describe the effect of molecular weight on the interfacial tension for linear materials. The power-law parameter was found to be numerically equivalent for that obtained for the molecular weight dependence of linear materials. The measured interfacial tension was also found to be dependent on the type of comonomer used in the PP-POE systems. The interfacial tension ranged from  $1.07 \pm 0.09$  dyn cm for a PP-POE system made using ethylene-propylene down to  $0.56 \pm 0.07$  dyn cm for a PP-POE made using ethylene-octene (24% octene).

## REFERENCES

1. S. Y. Hobbs, M. E. J. Dekkers, and V. H. Watkins, *Polymer*, **29**, 1598 (1988).
2. D. R. Paul and S. Newman, *Polymer Blends*, Vols. I and II, Academic Press, New York, 1978.
3. S. Wu, *Polym. Eng. Sci.*, **30**, 753 (1990).
4. G. I. Taylor, *Proc. Royal Soc., London*, **146A**, 501 (1934).
5. G. I. Taylor, *Proc. Royal Soc., London*, **226A**, 34 (1954).
6. S. Wu, *Polym. Eng. Sci.*, **27**, 335 (1987).
7. G. Serpe, J. Jarrin, and F. Dawans, *Polym. Eng. Sci.*, **30**, 553 (1990).
8. H. van Oene, *J. Coll. Interf. Sci.*, **40**, 448 (1972).
9. P. C. Ellingson, D. A. Strand, A. Cohen, R. L. Sammler, and C. J. Carriere, *Macromolecules*, **27**, 1643 (1994).
10. G. L. Gaines Jr. and G. L. Gaines III, *J. Coll. Interf. Sci.*, **63**, 394 (1978).
11. D. G. LeGrand and G. L. Gaines Jr., *J. Coll. Interf. Sci.*, **50**, 272 (1975).
12. S. H. Anastasiadis, I. Gancarz, and J. T. Koberstein, *Macromolecules*, **21**, 2980 (1988).
13. C. I. Poser and I. C. Sanchez, *J. Coll. Interf. Sci.*, **69**, 539 (1979).
14. C. I. Poser and I. C. Sanchez, *Macromolecules*, **14**, 361 (1981).
15. J. W. Cahn and J. E. Hillard, *J. Chem. Phys.*, **28**, 258 (1958).
16. S. K. Kumar, M. Vacatello, and D. Y. Yoon, *Macromolecules*, **23**, 2189 (1990).
17. C. J. Carriere, A. Cohen, and A. Arends, *J. Rheol.*, **33**, 681 (1989).
18. C. J. Carriere and A. Cohen, *J. Rheol.*, **35**, 205 (1991).
19. A. Cohen and C. J. Carriere, *Rheol. Acta*, **28**, 223 (1989).
20. R. L. Sammler, R. P. Dion, C. J. Carriere, and A. Cohen, *Rheol. Acta*, **31**, 554 (1992).
21. K. Kirjava, T. Rundqvist, R. Holsti-Miettinen, M. Heino, and T. Vainio, *J. Appl. Polym. Sci.*, **55**, 1069 (1995).
22. H. Edwards, *J. Appl. Polym. Sci.*, **12**, 2213 (1968).
23. T. Sakai, *Polymer*, **6**, 659 (1965).
24. S. Wu, *J. Coll. Interf. Sci.*, **C31**, 153 (1969).
25. S. Wu, *J. Polym. Sci.*, **C34**, 19 (1971).
26. R. J. Roe, *J. Coll. Interf. Sci.*, **C31**, 228 (1969).